Published in final edited form as:
Biochim Biophys Acta. 2011 March ; 1810(3): 317–329. doi:10.1016/j.bbagen.2010.05.004.

MULTI-STAGE DELIVERY NANO-PARTICLE SYSTEMS FOR THERAPEUTIC APPLICATIONS

Rita E. Serda[a], **Biana Godin**[a], **Elvin Blanco**[a], **Ciro Chiappini**[b], and **Mauro Ferrari**[*,a,b,c,d]

[a]University of Texas Health Science Center, Department of NanoMedicine and Biomedical Engineering, 1825 Pressler, Suite 537, Houston, TX 77030, USA

[b]University of Texas at Austin, Department of Biomedical Engineering, 1 University Station, C0400, Austin, TX 78712

[c]University of Texas MD Anderson Cancer Center, Department of Experimental Therapeutics, Unit 422, 1515 Holcombe Blvd., Houston, TX 77030, USA

[d]Rice University, Department of Bioengineering, Houston, TX 77005, USA

Abstract

Background—The daunting task for drug molecules to reach pathological lesions has fueled rapid advances in Nanomedicine. The progressive evolution of nanovectors has led to the development of multi-stage delivery systems aimed at overcoming the numerous obstacles encountered by nanovectors on their journey to the target site.

Scope of Review—This review summarizes major findings with respect to silicon-based drug delivery vectors for cancer therapeutics and imaging. Based on rational design, well established silicon technologies have been adapted for the fabrication of nanovectors with specific shapes, sizes, and porosities. These vectors are part of a multi-stage delivery system that contains multiple nano-components, each designed to achieve a specific task with the common goal of site-directed delivery of therapeutics.

Major Conclusions—Quasi-hemispherical and discoidal silicon microparticles are superior to spherical particles with respect to margination in the blood, with particles of different shapes and sizes having unique distributions *in vivo*. Cellular adhesion and internalization of silicon microparticles is influenced by microparticle shape and surface charge, with the latter dictating binding of serum opsonins. Based on *in vitro* cell studies, the internalization of porous silicon microparticles by endothelial cells and macrophages is compatible with cellular morphology, intracellular trafficking, mitosis, cell cycle progression, cytokine release, and cell viability. *In vivo* studies support superior therapeutic efficacy of liposomal encapsulated siRNA when delivered in multi-stage systems compared to free nanoparticles.

Keywords

Multi-stage vectors; drug delivery; microparticle; porous silicon; nanoparticle

[*]**To whom correspondence should be addressed: Mauro Ferrari**, University of Texas Health Science Center, Department of NanoMedicine and Biomedical Engineering, 1825 Pressler Street, Suite 537, Houston, TX 77030, USA, Phone: 713-500-2444; Mauro.Ferrari@uth.tmc.edu.

1. Introduction

Nanotechnology pertains to synthetic, engineerable objects which are nanoscale in dimensions or have critical functioning nanoscale components, leading to novel, unique properties [1–2]. These emergent characteristics arise from the material's large surface area and nanoscopic size [3]. Nanotechnology now occupies a niche as a burgeoning and revolutionary field within medicine known as nanomedicine, particularly within the field of oncology [1]. One of the potential benefits of nanomedicine is the creation of nanoparticle based vectors that deliver therapeutic cargo in sufficient quantity to a target lesion to enable a selective effect. This is a daunting task for all drug molecules, owing to the highly organized array of 'biological barriers' that the molecules encounter [3–6]. The human body presents a robust defense system that is extremely effective in preventing injected chemicals, biomolecules, nanoparticles and any other foreign agents from reaching their intended destinations. Biobarriers are sequential in nature, and therefore, the probability of reaching the therapeutic objective is the product of individual probabilities of overcoming each barrier [7–8]. Sequentially, with respect to intravascular injections, these comprise: enzymatic degradation; sequestration by phagocytes of the reticulo-endothelial system (RES) [9–10]; vascular endothelia [11]; adverse oncotic and interstitial pressures in the tumor [12–13]; cellular membranes, or subcellular organelles such as the nucleus and endosomes [14–15]; and molecular efflux pumps [16]. Without an effective strategy to negotiate these barriers, new or current therapeutic agents based on enhanced biomolecular selectivity may yield sub-optimal utility, simply because they reach the intended targets in very small fractions, with only 1 in 10,000 to 1 in 100,000 molecules reaching their intended site of action [7]. Due to this narrow therapeutic window, marginal tolerability and considerable mortality ensue [17]. Transport through different compartments and across biological barriers can be enhanced by optimization of particle size, shape, density and surface chemistry. These parameters dominate transport in the bloodstream, margination, cell adhesion, selective cellular uptake, and sub-cellular trafficking.

An early obstacle for intravascularly administered therapeutics is the endothelial wall which forms the boundary between the circulatory system and tissue specific microenvironments. Specific adherence of delivery vectors to diseased vasculature provides a key to conquering this early barrier, as does the hijacking of cells bound for the inflammatory microenvironment of the lesion. In order to efficiently overcome various biobarriers multiple levels of targeting, spatial release of secondary carriers or therapeutics, simultaneous delivery of independent systems or systems with a synergistic impact should be considered. The purpose of this review is to present the multi-stage concept of drug delivery and to summarize the experimental techniques and research findings that have transpired from this area of research.

2. Nanovector taxonomy

A variety of nanocarrier-based drug delivery systems with different compositions, geometry, and surface modifications are under various stages of investigation [1,18], producing an enormous collection of nanoparticles with a large array of possible combinations. Figure 1 illustrates three main categories of nanovectors that have been described based on their functions and capabilities [1,19–20]. First generation nanovectors are the most elementary, and home to diseased sites by passive mechanisms such as the enhanced permeation and retention (EPR) effect, or more specifically, extravasate through gaps in tumor neo-vasculature. Avoidance of uptake by the RES is through functionalization with neutral polymers, such as poly(ethylene glycol) (PEG) [21–23]. Interactions between the aqueous environment and the hydrophilic polymers permits extension and mobility of the polymeric

chains [24]. Derivatized nanoparticles adsorb plasma components more slowly [25] based on steric repulsion forces [26], negating opsonin driven uptake of nanoparticles by phagocytic cells, and enhancing blood circulation time. Advantages of nanoparticle-based carriers include improved delivery of water insoluble drugs, prolonged circulation half life, and reduced immunogenicity [27–28].

The second category of nanovectors is comprised of delivery systems with an additional functionality [29–33], including: (a) targeting of the disease site through ligands that specifically bind to receptors uniquely- or over-expressed in the tumor microenvironment; (b) advanced functionalities, including co-delivery of multiple therapeutics or imaging agents, or triggered or controlled release of therapeutic agents. More sophisticated than their predecessors, the second generation of nanovectors represents a progressive evolution of first-generation nanovectors.

The third generation of nanovectors represents a paradigm shift in the strategy to overcome numerous obstacles encountered by nanovectors on their journey to the target site. Since no single agent can conquer the plethora of barriers that exist, these nanovectors are comprised of diverse families of nanoparticles nested into a single vector to achieve collaborative interactions. These carriers, or Logic Embedded Vectors (LEVs) [8], are therapeutic, multi-component constructs specifically engineered to avoid biological barriers, in which the functions of biorecognition, cytotoxicity and biobarrier avoidance are decoupled, yet act in efficacious, operational harmony. As an example of this therapeutic strategy, one can envision a vector which effectively navigates through the vasculature based on its geometry, attaches to the diseased vascular site through specific surface recognition and releases different nanoparticle payloads that simultaneously and synergistically extravasate, reach tumor cells and deliver their active agents at optimal concentrations to selectively eliminate malignancy with minimal side effects. This concept describes the multi-stage delivery system that will be extensively reviewed in this paper. By definition, third generation nanovectors have the ability to perform a time sequence of functions through the use of multiple nano-based components that synergistically provide distinct functionalities.

In addition to the multi-stage delivery system, an example of third generation nanoparticles is biologically active molecular networks called “nanoshuttles”, which are self-assemblies of gold nanoparticles within a bacteriophage matrix. Nanoshuttles combine the hyperthermic response of a near-infrared or radiofrequency external energy of the gold with the biological targeting capabilities of the 4C-RGD sequence presented by the phage [32,34]. These nanoshuttles collectively accommodate enhanced fluorescence, dark-field microscopy, and surface-enhanced Raman scattering detection.

Another example of a third generation nanovectors is the “nanocell”, based on a disease-inspired approach to therapy. [35]. Utilizing the combinatorial chemotherapy approach, researchers have developed a nested nanoparticle construct that comprises a lipid-based nanoparticle enveloping a polymeric nanoparticle core called a “nanocell”. A conventional chemotherapeutic drug, doxorubicin, is conjugated to a polymer core and an anti-angiogenic agent, combretastatin, is then trapped within the lipid envelope. When nanocells accumulate within the tumor through the EPR effect, the sequential time release of the anti-angiogenic agent, and then the cytotoxic drug, causes an initial disruption of tumor vascular growth and effectively traps the drug conjugated nanoparticle core within the tumor to allow eventual delivery of the cancer cell killing agent.

Silica and silicon-based delivery systems represent the final example of third generation nanovectors. Mesoporous silica nanoparticles have been developed to co-deliver doxorubicin and Bcl-2 siRNA by encapsulation of doxorubicin inside the pores and

complexation of siRNA in a dendrimer shell [36]. The goal of this nanodevice is to simultaneously deliver an anticancer drug as an apoptosis inducer and siRNA molecules as suppressors of membrane pumps that mediate multidrug resistance. This multi-component nanodevice was able to significantly enhance the cytotoxicity of doxorubicin by decreasing the IC_{50} 64-fold.

Mesoporous silicon devices include our multi-stage system [37]. Based on well established semiconductor microfabrication lithography techniques, which allow for exquisite control of size, shape, and porosity, in concert with active biological targeting moieties, these vectors are intended to deliver large payloads of nanoparticles and higher order therapeutic and imaging agents to the tumor site. The “stage one” mesoporous silicon microparticles are designed based on mathematical modeling to exhibit superior margination and adhesion during their navigation through the systemic circulation. Stage one particles shoulder the burden of efficiently transporting, shielding, and controlling the rate of release of the nanoparticle payload. The encapsulated nanoparticles, called “stage two” nanoparticles, can be any nanovector construct within the approximate diameter range of 5–100 nm. The multi-stage drug delivery system is an example of LEVs which strategically combine numerous nano-components aimed at delivering single or multiple component nanovectors to the tumor site. The stage one particle is rationally designed to have a hemi-spherical or discoidal shape to enhance particle margination within the blood, as well as interactions between particles and endothelia, with a goal of maximizing the probability of active tumor targeting and adhesion [107]. In addition to improved hemodynamic properties and active biological targeting utilizing nano-components such as aptamers and phages, as will be discussed below, the stage one particles may also present specific surface modifications to avoid RES uptake. Following recognition of tumor vasculature and firm vascular adhesion, a series of nanoparticle payloads may be released in a sequential order dictated by diffusion from expanding or newly opened nanopores. Factors governing nanoparticle release include stage one particle degradation rates, polymeric coating, and stage two design strategies (e.g., environmentally sensitive cross-linking techniques with pH, temperature, and/or enzymatic triggers). We have observed that the degradation rate of the porous silicon particles is proportional to its porosity, and can be tuned from hours to days without surface functionalization. The versatility of this multi-stage delivery platform allows for a theranostic approach to therapy, including the delivery of chemotherapeutics, remotely activated hyperthermic nanoparticles, image contrast agents, and sequential, sustained release of successive stages of nanoparticle and active agents.

3. Rational design of stage one particles

The rational design of nanovectors aims at finding the dominating governing parameters in a series of events which are encountered as the particle travels from the site of administration to the intended site of action. Multi-stage vectors are transported in the blood stream, interact with the vascular endothelium, and eventually interact with endothelia in the tumor neovasculature. These three fundamental events in the intravascular “journey” provide the basis for rational design, including: (1) the margination dynamics, (2) firm adhesion, and (3) control of internalization. The term ‘margination’ is used in physiology to describe the lateral drift of white blood cells and platelets from the center of the blood vessels towards the endothelial walls. The rational design of particles aims at generating a marginating particle that can spontaneously move preferentially in close proximity to the blood vessel endothelium [38–39]. Unlike spherical particles, non-spherical particles exhibit more complex motions with tumbling and rolling which can be exploited to control their margination dynamics without any need for lateral external forces. The longitudinal (drag) and lateral (lift) forces, as well as the torque exerted by flowing blood, depend on the size, shape, and orientation of the particle, as well as the stream direction and vascular changes

that the particle encounters as it transverses through the bloodstream. For example, if one considers an elongated particle with an aspect ratio of 2, the particle motion becomes very complex with periodic oscillations towards and away from the wall [38]. Overall, however, the particle tends to approach the wall and periodically interact with its surface. More recently, in-vitro experiments conducted using spherical, discoidal and quasi-hemispherical particles with the same weight injected into a parallel plate flow chamber under controlled hydrodynamic conditions have shown that discoidal particles tend to marginate more than quasi-hemispherical particle, and both of these marginate more than spherical particles (Figure 2) [40–41]. It was also shown that the probability of adhesion is decreased as a result of increasing shear stress at the vessel wall and particle size. Cellular adhesion increases as the surface density of ligand molecules on the particle surface and receptor molecules on the cell membrane increase. For all particle shapes, a characteristic size can be identified for which the probability of adhesion has a maximum. [42]. For example, hydrodynamic forces decrease as particle size decreases, but the area of interaction at the particle/cell interface is also reduced, leading to fewer ligand-receptor interactions and reduced potential to withstand even small dislodging forces. For larger particles, the number of ligand-receptor bonds increases, but so do the hydrodynamic forces on the particles. With respect to particle adhesion, rational design seeks to optimize binding strength by modulation of particle shape and a balance between ligand surface density and binding affinity.

There are different mechanisms *in vivo* which govern the behavior of particles. Recent studies have demonstrated that particles of different shape have unique biological distributions (Figure 3) [43]. Six hours after systemic injection in mice, hemispherical particles accumulated preferentially in the liver, with minimal distribution to the heart and lungs, while discoidal particles showed relatively less retention in the liver, and high accumulation in the heart and lungs, as well as the spleen. Approximately 2% of the hemispherical particles accumulated in the tumor, which is significantly [43] greater than 1 in 10,000 (0.01%) biomolecularly targeted therapeutic agents. *In vivo* studies recently published support superior therapeutic efficacy of multi-stage delivered liposomal siRNA over first generation siRNA liposomes [44]. In this work, a single injection of siRNA in a multi-stage construct resulted in gene silencing equivalent to six injections of liposomal siRNA delivered over three weeks. These findings suggest that higher level targeting is achieved by second-stage vectors and/or therapeutic agents, perhaps by means of sustained, long term release of secondary agents from the first stage porous silicon vector.

There have been significant improvements in tumor accumulation (2–25 times higher) and therapy with PEGylated liposomal agents currently in clinical use as compared to non sterically- stabilized liposomes and to the free drug [45]. However, numerous reports state that the main fraction of the drug still accumulates in the filtering organs, with therapeutic loss of the drug [46–47]. With the multi-stage system, a comparable fraction of the multi-stage vector reaches the tumor; moreover, the fraction captured in the filtering organs is not therapeutically “lost”. As demonstrated in the multistage siRNA therapy study, porous silicon carriers trapped in the filtering organs slowly released second stage particles which were then able to migrate to target tissue, efficiently suppressing tumor growth for more than 21 days.

4. Fabrication of geometrically diverse stage one silicon particles

First stage nanoporous silicon particles are fabricated according to the edict of rational design for optimal performance, including: 1) Margination and adhesion; 2) Loading with Stage two nanoparticles; and 3) Control of degradation and release of secondary nanoparticles. Particles with determined size, shape and porous structure can be fabricated through a combination of photolithographic techniques and electrochemical etch [48–49]

(Figure 4). A thin masking layer of SiN is deposited on the silicon substrate, followed by spinning for photoresist development. The photoresist is patterned with the desired photomask and the pattern is transferred into the substrate by dry reactive ion etch. The substrate is then selectively porosified according to the lithographic pattern by anodic electrochemical etch in a solution of hydrofluoric acid and ethanol to obtain porous silicon particles that can be released from the substrate. The resulting particle maintains a central nucleation site in the size and shape of the photolithographic pattern, surrounded by an external corona whose thickness is determined by the electrochemical etch. This straightforward process can be controlled at each step to fine tune the physical properties of the resulting particle. Choosing the size and shape of the photolithographic pattern determines the size and shape of the particle nucleation site, influencing the overall size and shape. Our group has successfully fabricated particles with a circular nucleation site of size ranging from 400 nm to over 5 μm. The timing and gas composition of the dry reactive ion etch controls the depth and shape of the trenches formed in the silicon substrate, determining the aspect ratio and the profile of the resulting porous silicon particle. Shorter etch time creates shallow, high aspect ratio (up to 6) discoidal particles; while longer etch times yield thicker, quasi-hemispherical particles with aspect ratios ranging from 1 to 2. The substrate resistivity and doping type, timing, current density and solution composition during the electrochemical etch determine the thickness of the porous layer, the pore size and particle morphology[48–51]. Increasing resistivity, larger currents, and higher concentrations of ethanol with respect to hydrofluoric acid all contribute to the increase in pore size. Pore size larger than 20 nm is associated with straight, unbranched pores, while pores in the 10–20 nm size range show a branched tree-like structure. Pores smaller than 10 nm yield a randomly oriented network structure.

5. Loading porous silicon particles with second stage nanoparticles

Pore size and morphology affect particle loading, payload retention, and release kinetics [37]. We have shown that particles with 5 nm diameter pores can be loaded efficiently with 2×30 nm Single Wall Carbon Nanotubes (SWNTs), while 5 nm CdSe Quantum Dots (Qdots) are associated solely with the particle surface. Conversely, particles with 20 nm pores are capable of loading both SWNTs and the Qdots within the porous structure [37]. We have demonstrated sustained release of both Qdots and SWNTs from 20 nm pores over the course of 24 hr.

Success at loading secondary nanoparticles into the porous silicon matrix is best achieved using dry silicon particles. Loading then occurs by adding a concentrated solution of nanoparticles that is pulled into the pores by capillary action, i.e. the incipient wetness method [52–54]. Optimization of loading takes into account pore size, dimensions of the payload, surface charge or functionalization, and solvent optimization.

Alternately, loading has been achieved by covalent attachment of nanoparticles to the silicon surface. Successful loading has been demonstrated with 3-aminopropyltriethoxysilane (APTES) modified silicon microparticles and carboxylated iron oxide and gold nanoparticles using Sulfo-N-hydroxysuccinimide and 1-ethyl-3-(3-dimethylaminopropyl) carbodiimide chemistry. Scanning electron micrographs, displayed in Figure 5, show quasi-hemispherical silicon microparticles covalently loaded with gold nanoparticles (6 nm core) before (top left) and following cellular uptake (top right). The accompanying 3-(4,5-dimethylthiazol-2-yl)-2,5-diphenyl tetrazolium bromide (MTT) proliferation assay shows similar rates of cell growth in the presence of control or gold loaded porous silicon particles at ratios of 5 and 10 silicon particles per cell.

6. Targeting

Advances in tumor targeting have turned Paul Ehrlich's once-outlandish concept of a "magic bullet," where malignancies in the body can be treated by chemical substances equipped with high affinity for that malignancy,[55] into a very attainable goal. Thanks to significant strides in research concerning phage display libraries, it is now feasible to increase the affinity of nanoparticles for specific targets in these diseased states. This in turn results in increased amounts of nanoparticles concentrated at the site of action, permitting drug or imaging agents to exert their effects locally. In the case of targeted chemotherapeutics, enhanced efficacies result, and toxicity to healthy tissues and organs is substantially reduced. With regard to imaging agents, the increased amassing of nanoparticles at the site of action allows for enhanced contrast and proper delineation of tumor boundaries. In light of the overwhelming benefits of active targeting, the attachment of ligands to the surface of nanoparticles is presently an area of intense research. The ligands currently under active exploration, and those with the most clinical potential, include the following: peptides, thioaptamers, small organic compounds, carbohydrates, and antibodies.

During the process of angiogenesis and vascular remodeling in tumors, endothelial cells demonstrate an over expression of cell surface markers critical for cell proliferation and invasion, leading to lesion specific "zipcodes", or vascular addresses. These markers include several receptors and integrins, the principle ones being vascular endothelial growth receptor (VEGF) and the $\alpha_v\beta_3$ integrin [56]. Given their over expression on the surface of tumor vasculature endothelia, as well as the fact that blood is in constant contact with endothelial cells, these receptors and integrins are very attractive markers for tumor targeting. Phage display technology is used to map vascular zipcodes, that is, protein interacting sites. The benefits of phage technology include genetic manipulation, high throughput screening, and production in high titers (via propagation in host bacteria) [57]. Libraries of peptides are displayed on the surface of bacteriophage, then tested against target cells or *in vivo*, leading to isolation of target specific peptides by multiple rounds of "biopanning". Bound peptides are recovered and the sequence is screened against databanks to identify sequence homology with existing motifs. For example, the RGD-4C peptide, isolated by *in vivo* phage display, is currently being used as a tumor homing peptide for first stage vectors via targeting of integrins.

Gao and coworkers were able to conjugate a cyclic Arg-Gly-Asp-D-Phe-Lys (cRGD) peptide to the surface of polymer micelles that encapsulated superparamagnetic iron oxide nanoparticles [58]. Once administered intravenously, the polymer micelles were able to actively target A549 lung tumors implanted subcutaneously in mice, leading to enhanced tumor imaging under MRI as compared to non-targeted micelles.

Another option for targeting includes aptamers, oligonucleotide molecules that are selected based on their affinity for the native tertiary structure of target molecules expressed on the cell surface [59]. Modification of one or both of the phosphoryl non-bridging oxygen atoms of the aptamer with sulfur creates "thioaptamers" with increased resistance to nucleases, tighter binding, and reduced negative charge leading to enhanced cellular uptake of aptamer decorated nanoparticles. The aptamers can be thio-modified enzymatically and the resulting oligonucleotides have been shown to be rapidly cleared by the renal system. Hybrid thioaptamers, with a mix of thiophosphate and unmodified phosphate are the best option for specificity, nuclease resistance, and high affinity.

Ramakrishnan and coworkers showed that a VEGF-toxin conjugate ($VEGF_{165}$-DT_{385}), administered intraperitoneally, was able to target a subcutaneous human ovarian cancer cell xenograft (MA148) in mice, leading to tumor growth delay.[60] Cheresh and coworkers

synthesized a cationic polymer lipid-based nanoparticle fashioned with a small organic $\alpha_v\beta_3$ ligand [61]. After 24 hours, these nanoparticles, which also contained a gene encoding firefly luciferase, were observed in human melanoma cells over expressing $\alpha_v\beta_3$. It is important to note that nanoparticles were rarely observed in healthy organs and tissues.

Folic acid represents a small organic molecule used for tumor targeting, given that the receptor for folic acid is a protein overexpressed in many different cancer cells [62]. Doxorubicin polymer micelles fashioned with folic acid, developed by Park et al., showed increased uptake in KB cells *in vitro*, with *in vivo* work showing a significant decrease in tumor growth rate when compared to non-targeted micelles [63]. Carbohydrate molecules have been used to target hepatocellular carcinoma, given the overexpression of the asialoglycoprotein receptor (ASGPR), a membrane lectin receptor, on these cells [64]. The most studied carbohydrate molecules for targeting include galactose and lactose. Cho et al. demonstrated a 30% increase in paclitaxel-loaded polymer micelles in cells overexpressing ASGPR as compared to cells that did not express the receptor [65].

Monoclonal antibodies, which possess high binding affinities, are also actively being explored as tumor-specific targeting modalities. Trastuzumab, a humanized monoclonal antibody specific for the HER2/neu receptor (erbB2), is an FDA approved drug used for the treatment of HER2-positive breast cancer [66]. Trastuzumab causes cell cycle arrest leading to decreased cancer cell proliferation and reduced angiogenesis. Antibodies specific for HER2 have been used as targeting ligands for selective delivery of silica gold nanoshells to tumor tissue [67]. Other antibody-based targeting agents include monoclonal antibodies specific alphavbeta3 [68], which when covalently coupled to human serum albumin nanoparticles, resulted in enhanced binding to melanoma cells. Monoclonal antibodies against alphavbeta3 integrin were also shown to inhibit both cancer growth and angiogenesis [68].

7. Therapeutic applications of multi-stage delivery systems

Nanotechnology is projected to fill the gap between significant scientific advances in the areas of cancer imaging and diagnosis, discovery and development of a plethora of anticancer drugs, and their translation into improvements in cancer management. With optimal anticancer treatment regimens still lacking, novel therapeutic approaches are being explored to supplement or replace traditional gold standards, including surgical resection [69] and radiation therapy [70]. While the curative potential of anticancer drugs is indisputable, limitations that hinder clinical translation and success include nonspecific drug delivery. In this section, we describe various “stage two” nanoparticles that have been successfully incorporated in the multi-stage system for various therapeutic applications.

7.1 Liposomes

Liposomes represent a nanotherapeutic modality that shows immense clinical potential for drug delivery. These vesicular nanostructures, formed from phospholipid and cholesterol molecules, possess several advantages for drug delivery. First, their inner hydrophilic compartment can encapsulate water-soluble drugs, as well as therapeutic proteins, DNAs, and siRNAs. Second, with a diameter in the range of 100 nm, the drug payload can be substantial. Lastly, their functionalizaton with PEG can grant them with stealth-like properties, avoiding uptake by the RES. The chief disadvantage to liposomal drug delivery is the inability to encapsulate poorly soluble drugs within the aqueous core, limiting encapsulation of drugs to the hydrophobic bilayer membrane. A PEGylated liposomal formulation, known as Doxil®, is currently in clinical trials for the treatment of Kaposi’s sarcoma [71]. These stealth liposomes have long blood circulation times over non-PEGylated liposomes, and readily accumulate in tumors due to passive targeting [72–73].

Another drug that was successfully encapsulated in liposomes is annamycin, a non-cross-resistant anthracycline [74]. The pre-liposomal annamycin lyophilized powder contains phospholipids (dimyristoylphosphatidyl choline and dimyristoylphosphatidyl glycerol at a 7:3 molar ratio), annamycin (lipid:drug at a ratio 50:1 w/w), and Tween 20. The surfactant in the formulation allows for better solubilization of the drug, shortening the reconstitution step, as well as a means to form nano-size carriers without destroying the liposomal structure [75]. Similar to doxorubicin, the drug possesses native fluorescence in the red region. In Figure 6, we show flow cytometry data supporting loading of annamycin liposomes into porous silicon microparticles. Loading resulted in a shift in the mean fluorescent intensity from 3 to 1285 AU. Other liposomal active agents that were successfully loaded into the multi-stage drug delivery system include paclitaxel, doxorubicin and siRNA. *In vitro* and *in vivo* efficacy studies with these systems in various cancer models are underway.

7.2 Polymer micelles

Ringsdorf and coworkers worked in the early 1980s on the development of polymer micelles as drug delivery vehicles [76]. These spherical, supramolecular constructs, with a size ranging from 10–100 nm, are formed from the self-assembly of biocompatible amphiphilic block copolymers in aqueous environments [77–79]. The hydrophilic outer portion, typically composed of PEG, forms a hydrating layer, while the hydrophobic core, composed of polymers such as poly(D,L-lactic acid) (PDLLA), poly(ε-caprolactone) (PCL), and poly(propylene oxide) (PPO), houses the anticancer agent. The ability of the drug to be encapsulated within the hydrophobic core represents their main advantage, in addition to their innate possession of a PEG hydrophilic corona that prevents opsonization and RES uptake [80], and their small size which leads to their preferential accumulation in tumor tissue through the EPR effect.

Currently, several polymeric micelle platforms are being explored in clinical trials. Kataoka and coworkers formulated doxorubicin-containing poly(ethylene glycol)–poly(L-aspartic acid) micelles [79]. This formulation, known as NK911, displayed long blood circulation times and nearly tripled the half-life of doxorubicin [81]. Genexol-PM is another micelle formulation in clinical trials, and consists of PEG-PLA micelles that encapsulate paclitaxel. Findings showed that Genexol-PM was much more tolerable than the clinically used formulation of paclitaxel containing Cremephor® EL, a formulation that results in hypersensitivity reactions [82]. As a result, the dose of paclitaxel administered to patients could be increased, which in turn resulted in enhanced anti-tumor efficacy in patients [83–84].

To further enhance selective delivery of chemotherapeutics to the lesion, doxorubicin and paclitaxel polymeric micelles have been loaded into the nanoporous matrix of the silicon microparticles (data not shown). For doxorubicin the best loading was obtained with 1,2-distearoyl-phosphatidyl ethanolamine-methyl-poly(ethyleneglycol) anionic micelles loaded into oxidized porous silicon microparticles. *In vivo* efficacy studies for cancer therapy are currently underway.

8. Biocompatibility

8.1 Directed opsonization of silicon microparticles

The composition and physical characteristics of particles influences both their physical properties [85–86] (e.g. electromagnetic), and their biological attributes [87–88]. Size, shape, chemical composition, and surface charge all strongly influence the impact nano- and micron-size particles have on cellular systems, leading to differences in biocompatibility. To explore the biological properties of our stage one porous silicon microparticles, the impact

of particles of different sizes and surface modifications on interactions with macrophages and endothelial cells has been characterized.

For therapeutic and imaging applications, nanoparticles and microparticles may be administered intravenously. During transport in the blood stream, these particles become coated with serum components that adsorb to the particle surface. Associations between cells and particles are regulated in part by serum proteins adsorbed to the nanoparticle surface. These surface-bound components are referred to as either opsonins or dysopsonins, depending on their impact, which either favor or disfavor cellular binding and uptake. One method to reduce serum protein binding is to coat particles with a neutral polymer that reduces cellular uptake, such as PEG. A second strategy is to alter the particle surface to attract serum components that enhance binding to target cell populations [87].

As previously stated, the target of stage one nanoporous silicon microparticles is diseased vasculature. As previously discussed, during many pathological states, including cancer, inflammation alters surface moieties expressed on vascular endothelia. To simulate inflammatory conditions *in vitro*, endothelial cells were treated with TNF-α for 48 hr and the impact on cellular association with silicon microparticles was monitored by using the increase in orthogonal light scatter by cells upon association with particles as a metric for binding and cellular uptake. Serum components binding to oxidized silicon microparticles, as well as negatively charged polystyrene microparticles, inhibited particle association with endothelial cells, while factors binding to positive, APTES-modified silicon microparticles had no impact on microparticle association with endothelial cells. Stimulation with TNF- α further increased association of microparticles with endothelial cells. While opsonization of oxidized silicon microparticles with pure IgG similarly inhibited association with endothelial cells, it enhanced association with macrophages, which express receptors for immunoglobulin (e.g. FcγRII). These findings indicate that it may be possible to manipulate particle surface attributes to direct opsonization for selective targeting of cell populations.

8.2 Cellular engulfment of stage one silicon microparticles

Benefits of cellular uptake of drug delivery particles include cell specific killing, molecular imaging, altered gene or protein expression, protein modification, and transcellular transport. Cellular uptake of nanoporous silicon microparticles has been explored using real-time confocal microscopy, scanning electron microscopy, and flow cytometry in two subclasses of endothelial cells, Human Umbilical Vein Endothelial Cells (HUVECs) and Human MicroVascular Endothelial Cells (HMVECs) [89]. Initial experiments compared cellular uptake of labeled (Dylight-594; Pierce) versus label-free particles. Using flow cytometry-derived side scatter as a metric for cellular uptake of microparticles, cellular association with labeled particles was found to be equivalent to label-free particles. Similarly, labeling of cells with variable amounts of dyes (i.e. CellTracker Green; Invitrogen; 0.25–2 μM) did not impact cellular association with microparticles. Confocal imaging of a single cell demonstrated membrane expansion around a microparticle at approximately 5–7 min after particle contact with the cell [89].

In Figure 7, scanning electron micrographs show two sizes [1.6 (top row) and 3.2 (bottom row) μm] of porous silicon microparticles bound to the surface of HUVEC endothelial cells [88]. Pseudopodia, projecting from the cell surface, are seen “looping” around both 1.6 and 3.2 μm particles 15 min after introduction at 37°C. The membrane eventually spreads outward to engulf the microparticles, as evidenced for one microparticle in Figure 7B, which is seen oriented perpendicular to the cell membrane. Actin cup formation and engulfment of microparticles by endothelial cells are shown in transmission electron micrographs in Figure 8 [87]. Based on particle size (> 1 μm), outward membrane extension during uptake, and inhibition of uptake by Cytochalasin B [87], an inhibitor of actin polymerization, the

mechanism of uptake was shown to be phagocytosis. Macropinocytosis, a second actin-driven mechanism of cellular uptake involving membrane ruffle formation, also appears to play a role in cellular uptake of silicon microparticles [87].

To determine the kinetics for internalization of microparticles a double fluorescent/FRET based assay was developed [89]. Intermolecular FRET was found to occur between FITC and PE fluorophores when FITC-labeled antibody, bound to the surface of endothelial cells, was coupled with a secondary PE labeled antibody. Emission from the FITC fluorophore is quenched upon binding of the secondary antibody, and cells appear positive for the PE fluorophore only. Cells with both surface-bound (quenched, PE positive) and internalized (protected; FITC positive) microparticles, are positive for both FITC and PE. Cells containing only internalized microparticles are green (FITC positive) only. Using the double antibody assay, the time for internalization of half of the microparticles was 15.7 min. Using flow cytometry to measure cellular association with microparticles in the presence of different ratios of particles to cells, cellular association was found to be identical for HUVECs at passages 5 and 8, and for HMVECs [89].

8.3 Cellular compatibility of stage one porous silicon microparticles

In order to validate the biological safety of therapeutic devices, it is essential to evaluate normal biological processes and the effect of devices on these events. The biological impact of porous silicon vectors has been evaluated in two cell lines representing the immune system (i.e. macrophages) and a potential physiological target or barrier to delivery (i.e. endothelial cells). Cellular morphology, cell viability, impact on cell cycle, mitotic potential and pro-inflammatory responses following cellular engulfment of silicon microparticles have been demonstrated [88]. Both cell types internalize microparticles adhering to the cell surface by phagocytosis, with subsequent intracellular transport of vesicles to the perinuclear region of the cell [87]. Mitotic partitioning of endosomes during cellular mitosis is an event mediated by cytoskeletal processes. We have shown that endothelial cells with internalized silicon microparticles undergo normal cellular proliferation, and cells with as many as 30 internalized silicon microparticles display even partitioning of microparticle-bearing endosomes to daughter cells during mitosis (Figure 9) [88]. Figure 9 is a series of phase contrast confocal micrographs of unstained, live cells undergoing mitosis. The cells were imaged in five focal planes at 5 minute intervals for 19 hours and select still shots are presented. Completion of cytokinesis, the final stage of mitosis, is dependent on polarized delivery of endocytic recycling membranes, and the finding of polarized delivery of microparticle-bearing vesicles to daughter cells supports a non disruptive role for internalized microparticles. The number of microparticles per cell was also monitored as a function of time over six days. At each cell doubling time for HMVECs (48 hr) the number of microparticles per cell was reduced by 50%, supporting equal partitioning of microparticle-bearing vesicles over multiple mitotic events [88].

Undisturbed endothelial proliferation and lack of cytotoxicity following internalization of silicon microparticles was also supported by an MTT assay, which measures mitochondrial enzyme activity (Figure 5). Control silicon microparticles and those covalently loaded with either iron oxide (10 nm core) or gold (6 nm core) nanoparticles did not alter cellular proliferation of endothelial cells over 72 hrs. Similar data has been obtained for macrophages.

The impact of silicon microparticle internalization on cell cycle has been evaluated in endothelial cells using flow cytometry [88]. At 12 and 24 hr following microparticle introduction (10:1; microparticle:cell) DNA content, analyzed by propidium iodide staining, showed no difference in relative cell cycle composition compared to control cells. In contrast, cellular exposure to Cisplatin, a common chemotherapeutic agent, inhibited cellular

mitosis as evidenced by a reduction in the G2/M peak. Flow cytometry analysis of the apoptotic volume, that is, cells with cell volume loss or cell shrinkage, confirmed a major accumulation of cell fragments following Cisplatin treatment, but no evidence of cell death due to cellular uptake of microparticles.

Since foreign material can elicit an immune response, induction of cytokine release following exposure of endothelial cells to silicon microparticles has been assessed by measuring two pro-inflammatory cytokines, IL-6 and IL-8, in the cell media. While positive control zymosan particles elicited a prominent increase in cytokine production, no significant increase was seen after microparticle exposure for 1, 4, and 24 hr. In summary, studies to date have shown that endothelial cells are unaffected by the presence of porous silicon microparticles based on analysis of cell morphology, viability, cell cycle, apoptosis, and mitosis. Similarly, macrophages display no impairment of cellular function in the presence of silicon microparticles based on cell morphology, viability, and inflammatory response (data pending publication).

9. Conclusions

Multi-stage delivery systems exemplify the progressive evolution of nanovectors. Based on rational design, well established silicon technologies have been adapted for the fabrication of nanovectors with specific shapes, sizes, and porosities. These vectors are part of a multi-stage delivery system that contains multiple nano-components, each designed to achieve a specific task with the common goal of site-directed delivery of therapeutics to a target lesion. Quasi-hemispherical and discoidal silicon microparticles have been found to be superior to spherical particles with respect to margination in the blood, and particles of different shapes and sizes have unique distributions *in vivo*. Cellular adhesion and internalization of silicon microparticles is influenced by microparticle shape and surface charge, with the latter affecting binding by serum opsonins. The presence of inflammatory cytokines has been shown to enhance cellular uptake of silicon microparticles by both endothelial cells and macrophages. Based on *in vitro* studies, internalization of porous silicon microparticles is compatible with cellular morphology, intracellular trafficking, mitosis, cell cycle progression, cytokine release, and cell viability.

Abbreviations

MDS	multi-stage delivery system
PEG	poly (ethylene glycol)
MTT	3-(4,5-dimethylthiazol-2-yl)-2,5-diphenyl tetrazolium bromide
HMVEC	Human MicroVascular Endothelial Cell
HUVEC	Human Umbilical Vein Endothelial Cell
APTES	3-aminopropyltriethoxysilane
Qdots	quantum dots
RES	reticulo-endothelial system

Acknowledgments

The authors would like to thank members of the Ferrari Research Team for their scientific contributions. This research was supported by the Department of Defense, grants DODW81XWH-07-1-0596, DODW81XWH-09-1-0212 and DODW81XWH-07-2-0101; NASA NNJ06HE06A; NIH RO1CA128797, RC2GM092599, U54CA143837; and State of Texas, Emerging Technology Fund.

REFERENCES

1. Ferrari M. Cancer nanotechnology: opportunities and challenges. Nat Rev Cancer 2005;5:161–171. [PubMed: 15738981]
2. Theis T, Parr D, Binks P, Ying J, Drexler KE, Schepers E, Mullis K, Bai C, Boland JJ, Langer R, Dobson P, Rao CN, Ferrari M. nan'o.tech.nol'o.gy n. Nat Nanotechnol 2006;1:8–10. [PubMed: 18654128]
3. Riehemann K, Schneider SW, Luger TA, Godin B, Ferrari M, Fuchs H. Nanomedicine--challenge and perspectives. Angew Chem Int Ed Engl 2009;48:872–897. [PubMed: 19142939]
4. Jain RK. Delivery of novel therapeutic agents in tumors: physiological barriers and strategies. J Natl Cancer Inst 1989;81:570–576. [PubMed: 2649688]
5. Jain RK. Transport of molecules, particles, and cells in solid tumors. Annu Rev Biomed Eng 1999;1:241–263. [PubMed: 11701489]
6. Sakamoto J, Annapragada A, Decuzzi P, Ferrari M. Antibiological barrier nanovector technology for cancer applications. Expert Opin Drug Deliv 2007;4:359–369. [PubMed: 17683250]
7. Ferrari M. Nanovector therapeutics. Curr Opin Chem Biol 2005;9:343–346. [PubMed: 15967706]
8. Ferrari M. Frontiers in Cancer Nanomedicine: Transport Oncophysics and Logic-Embedded Vectors. Trends in Biotechnology. 2009 In press.
9. Caliceti P, Veronese FM. Pharmacokinetic and biodistribution properties of poly(ethylene glycol)-protein conjugates. Advanced drug delivery reviews 2003;55:1261–1277. [PubMed: 14499706]
10. Moghimi SM, Davis SS. Innovations in avoiding particle clearance from blood by Kupffer cells: cause for reflection. Critical reviews in therapeutic drug carrier systems 1994;11:31–59. [PubMed: 7704918]
11. Mehta D, Malik AB. Signaling mechanisms regulating endothelial permeability. Physiol Rev 2006;86:279–367. [PubMed: 16371600]
12. Stohrer M, Boucher Y, Stangassinger M, Jain RK. Oncotic pressure in solid tumors is elevated. Cancer research 2000;60:4251–4255. [PubMed: 10945638]
13. Less JR, Posner MC, Boucher Y, Borochovitz D, Wolmark N, Jain RK. Interstitial hypertension in human breast and colorectal tumors. Cancer research 1992;52:6371–6374. [PubMed: 1423283]
14. Torchilin VP. Recent approaches to intracellular delivery of drugs and DNA and organelle targeting. Annu Rev Biomed Eng 2006;8:343–375. [PubMed: 16834560]
15. Majumdar S, Mitra AK. Chemical modification and formulation approaches to elevated drug transport across cell membranes. Expert Opin Drug Deliv 2006;3:511–527. [PubMed: 16822226]
16. Undevia SD, Gomez-Abuin G, Ratain MJ. Pharmacokinetic variability of anticancer agents. Nature reviews 2005;5:447–458.
17. Canal P, Gamelin E, Vassal G, Robert J. Benefits of pharmacological knowledge in the design and monitoring of cancer chemotherapy. Pathol Oncol Res 1998;4:171–178. [PubMed: 9761935]
18. Wagner V, Dullaart A, Bock AK, Zweck A. The emerging nanomedicine landscape. Nat Biotechnol 2006;24:1211–1217. [PubMed: 17033654]
19. Sanhai WR, Sakamoto JH, Canady R, Ferrari M. Seven challenges for nanomedicine. Nat Nanotechnol 2008;3:242–244. [PubMed: 18654511]
20. Heath JR, Davis ME. Nanotechnology and cancer. Annu Rev Med 2008;59:251–265. [PubMed: 17937588]
21. Hashizume H, Baluk P, Morikawa S, McLean JW, Thurston G, Roberge S, Jain RK, McDonald DM. Openings between defective endothelial cells explain tumor vessel leakiness. Am J Pathol 2000;156:1363–1380. [PubMed: 10751361]
22. Maeda H. The enhanced permeability and retention (EPR) effect in tumor vasculature: the key role of tumor-selective macromolecular drug targeting. Adv Enzyme Regul 2001;41:189–207. [PubMed: 11384745]
23. Torchilin VP. Recent advances with liposomes as pharmaceutical carriers. Nat Rev Drug Discov 2005;4:145–160. [PubMed: 15688077]

24. Hrkach JS, Peracchia MT, Domb A, Lotan N, Langer R. Nanotechnology for biomaterials engineering: structural characterization of amphiphilic polymeric nanoparticles by 1H NMR spectroscopy. Biomaterials 1997;18:27–30. [PubMed: 9003893]
25. Senior J, Delgado C, Fisher D, Tilcock C, Gregoriadis G. Influence of surface hydrophilicity of liposomes on their interaction with plasma protein and clearance from the circulation: studies with poly(ethylene glycol)-coated vesicles. Biochim Biophys Acta 1991;1062:77–82. [PubMed: 1998713]
26. Owens DE 3rd, Peppas NA. Opsonization, biodistribution, and pharmacokinetics of polymeric nanoparticles. Int J Pharm 2006;307:93–102. [PubMed: 16303268]
27. Lee CC, MacKay JA, Frechet JM, Szoka FC. Designing dendrimers for biological applications. Nat Biotechnol 2005;23:1517–1526. [PubMed: 16333296]
28. Duncan R. The dawning era of polymer therapeutics. Nat Rev Drug Discov 2003;2:347–360. [PubMed: 12750738]
29. Brannon-Peppas L, Blanchette JO. Nanoparticle and targeted systems for cancer therapy. Adv Drug Deliv Rev 2004;56:1649–1659. [PubMed: 15350294]
30. Kale AA, Torchilin VP. "Smart" drug carriers: PEGylated TATp-modified pH-sensitive liposomes. J Liposome Res 2007;17:197–203. [PubMed: 18027240]
31. Farokhzad OC, Langer R. Impact of nanotechnology on drug delivery. ACS Nano 2009;3:16–20. [PubMed: 19206243]
32. Souza GR, Staquicini FI, Christianson DR, Ozawa MG, Miller JH, Pasqualini R, Arap W. Combinatorial targeting and nanotechnology applications. Biomed Microdevices. 2009
33. Juweid M, Neumann R, Paik C, Perez-Bacete MJ, Sato J, van Osdol W, Weinstein JN. Micropharmacology of monoclonal antibodies in solid tumors: direct experimental evidence for a binding site barrier. Cancer Res 1992;52:5144–5153. [PubMed: 1327501]
34. Souza GR, Christianson DR, Staquicini FI, Ozawa MG, Snyder EY, Sidman RL, Miller JH, Arap W, Pasqualini R. Networks of gold nanoparticles and bacteriophage as biological sensors and cell-targeting agents. Proc Natl Acad Sci U S A 2006;103:1215–1220. [PubMed: 16434473]
35. Sengupta S, Eavarone D, Capila I, Zhao G, Watson N, Kiziltepe T, Sasisekharan R. Temporal targeting of tumour cells and neovasculature with a nanoscale delivery system. Nature 2005;436:568–572. [PubMed: 16049491]
36. Chen AM, Zhang M, Wei D, Stueber D, Taratula O, Minko T, He H. Co-delivery of Doxorubicin and Bcl-2 siRNA by Mesoporous Silica Nanoparticles Enhances the Efficacy of Chemotherapy in Multidrug-Resistant Cancer Cells. Small. 2009
37. Tasciotti E, Liu X, Bhavane R, Plant K, Leonard AD, Price BK, Cheng MM, Decuzzi P, Tour JM, Robertson F, Ferrari M. Mesoporous silicon particles as a multistage delivery system for imaging and therapeutic applications. Nat Nanotechnol 2008;3:151–157. [PubMed: 18654487]
38. Decuzzi P, Ferrari M. Design maps for nanoparticles targeting the diseased microvasculature. Biomaterials 2008;29:377–384. [PubMed: 17936897]
39. Decuzzi P, Ferrari M. Modulating cellular adhesion through nanotopography. Biomaterials 2010;31:173–179. [PubMed: 19783034]
40. Gentile F, Chiappini C, Fine D, Bhavane RC, Peluccio MS, Cheng MM, Liu X, Ferrari M, Decuzzi P. The effect of shape on the margination dynamics of non-neutrally buoyant particles in two-dimensional shear flows. J Biomech 2008;41:2312–2318. [PubMed: 18571181]
41. Gentile F, Curcio A, Indolfi C, Ferrari M, Decuzzi P. The margination propensity of spherical particles for vascular targeting in the microcirculation. J Nanobiotechnology 2008;6:9. [PubMed: 18702833]
42. Lee SY, Ferrari M, Decuzzi P. Shaping nano-/micro-particles for enhanced vascular interaction in laminar flows. Nanotechnology 2009;20:495101. [PubMed: 19904027]
43. Decuzzi P, Godin B, Tanaka T, Lee SY, Chiappini C, Liu X, Ferrari M. Size and shape effects in the biodistribution of intravascularly injected particles. J Control Release. 2009
44. M.L. Tanaka T, Vivas-Mejia PE, Nieves-Alicea R, Mann AP, Mora E, Han H, Shahzad MMK, Liu X, Bhavane R, Gu J, Fakhoury JR, Chiappini C, Lu C, Matsuo K, Godin B, Stone RL, Nick AM, Lopez-Berestein G, Sood AK, Ferrari M. Sustained siRNA Delivery by Mesoporous Silicon Particles. Cancer Res forthcoming. 2010

45. Papahadjopoulos D, Allen TM, Gabizon A, Mayhew E, Matthay K, Huang SK, Lee KD, Woodle MC, Lasic DD, Redemann C, et al. Sterically stabilized liposomes: improvements in pharmacokinetics and antitumor therapeutic efficacy. Proc Natl Acad Sci U S A 1991;88:11460–11464. [PubMed: 1763060]

46. Hong RL, Huang CJ, Tseng YL, Pang VF, Chen ST, Liu JJ, Chang FH. Direct comparison of liposomal doxorubicin with or without polyethylene glycol coating in C-26 tumor-bearing mice: is surface coating with polyethylene glycol beneficial? Clin Cancer Res 1999;5:3645–3652. [PubMed: 10589782]

47. Klibanov AL, Maruyama K, Torchilin VP, Huang L. Amphipathic polyethyleneglycols effectively prolong the circulation time of liposomes. FEBS Lett 1990;268:235–237. [PubMed: 2384160]

48. Serda, CCRE.; Fine, D.; Tasciotti, E.; Ferrari, M. Porous silicon particles for imaging and therapy of cancer, Nanostructured Oxides. Kumar, CSSR., editor. Vol. 2. Wiley VCH Verlag GmbH&Co; 2009. p. 357-398.

49. Tasciotti JME, Chiappini C, Bhavane R, Ferrari M. Porous silicon particles for multi-stage delivery. Nanoscale Bioengineering and Nanomedicine 2009:235–271.

50. Herino GBR, Barla K, Bertand C. Porosity and pore size distributions of porous silicon layers. J Eectrochem Soc 1987;134:1994–2000.

51. Zhang XG. Morphology and formation mechanisms of porous silicon. J. Electrochem. Soc 2004;151:C69–C80.

52. Zhang X, Zhang C, Guo H, Huang W, Polenova T, Francesconi LC, Akins DL. Optical spectra of a novel polyoxometalate occluded within modified MCM-41. J Phys Chem B 2005;109:19156–19160. [PubMed: 16853470]

53. Boujday S, Blanchard J, Villanneau R, Krafft JM, Geantet C, Louis C, Breysse M, Proust A. Polyoxomolybdate-stabilized Ru(0) nanoparticles deposited on mesoporous silica as catalysts for aromatic hydrogenation. Chemphyschem 2007;8:2636–2642. [PubMed: 18058778]

54. Mellaerts R, Jammaer JA, Van Speybroeck M, Chen H, Van Humbeeck J, Augustijns P, Van den Mooter G, Martens JA. Physical state of poorly water soluble therapeutic molecules loaded into SBA-15 ordered mesoporous silica carriers: a case study with itraconazole and ibuprofen. Langmuir 2008;24:8651–8659. [PubMed: 18630936]

55. Winau F, Westphal O, Winau R. Paul Ehrlich--in search of the magic bullet. Microbes Infect 2004;6:786–789. [PubMed: 15207826]

56. Pasqualini R, Koivunen E, Ruoslahti E. Alpha v integrins as receptors for tumor targeting by circulating ligands. Nat Biotechnol 1997;15:542–546. [PubMed: 9181576]

57. Decuzzi P, Pasqualini R, Arap W, Ferrari M. Intravascular delivery of particulate systems: does geometry really matter? Pharm Res 2009;26:235–243. [PubMed: 18712584]

58. Khemtong C, Kessinger CW, Ren J, Bey EA, Yang SG, Guthi JS, Boothman DA, Sherry AD, Gao J. In vivo off-resonance saturation magnetic resonance imaging of alphavbeta3-targeted superparamagnetic nanoparticles. Cancer Res 2009;69:1651–1658. [PubMed: 19190328]

59. Thiviyanathan V, Somasunderam AD, Gorenstein DG. Combinatorial selection and delivery of thioaptamers. Biochem Soc Trans 2007;35:50–52. [PubMed: 17233599]

60. Olson TA, Mohanraj D, Roy S, Ramakrishnan S. Targeting the tumor vasculature: inhibition of tumor growth by a vascular endothelial growth factor-toxin conjugate. Int J Cancer 1997;73:865–870. [PubMed: 9399667]

61. Hood JD, Bednarski M, Frausto R, Guccione S, Reisfeld RA, Xiang R, Cheresh DA. Tumor regression by targeted gene delivery to the neovasculature. Science 2002;296:2404–2407. [PubMed: 12089446]

62. Weitman SD, Weinberg AG, Coney LR, Zurawski VR, Jennings DS, Kamen BA. Cellular-Localization of the Folate Receptor - Potential Role in Drug Toxicity and Folate Homeostasis. Cancer Research 1992;52:6708–6711. [PubMed: 1330299]

63. Yoo HS, Park TG. Folate-receptor-targeted delivery of doxorubicin nano-aggregates stabilized by doxorubicin-PEG-folate conjugate. J Control Release 2004;100:247–256. [PubMed: 15544872]

64. Wands JR, Blum HE. Primary hepatocellular carcinoma. N Engl J Med 1991;325:729–731. [PubMed: 1651454]

65. Jeong YI, Seo SJ, Park IK, Lee HC, Kang IC, Akaike T, Cho CS. Cellular recognition of paclitaxel-loaded polymeric nanoparticles composed of poly(gamma-benzyl L-glutamate) and poly(ethylene glycol) diblock copolymer endcapped with galactose moiety. Int J Pharm 2005;296:151–161. [PubMed: 15885467]

66. Tomadoni A, Lombardo D, Wainstein R. Trastuzumab in the treatment of advanced breast cancer. Our single-center experience and spotlights of the latest national consensus meeting. Medicina (B Aires) 2004;64:20–24. [PubMed: 15034952]

67. Carpin LB, Bickford LR, Agollah G, Yu TK, Schiff R, Li Y, Drezek RA. Immunoconjugated gold nanoshell-mediated photothermal ablation of trastuzumab-resistant breast cancer cells. Breast Cancer Res Treat. 2010

68. Wagner S, Rothweiler F, Anhorn MG, Sauer D, Riemann I, Weiss EC, Katsen-Globa A, Michaelis M, Cinatl J Jr, Schwartz D, Kreuter J, von Briesen H, Langer K. Enhanced drug targeting by attachment of an anti alphav integrin antibody to doxorubicin loaded human serum albumin nanoparticles. Biomaterials 2010;31:2388–2398. [PubMed: 20031203]

69. Finlayson EV, Goodney PP, Birkmeyer JD. Hospital volume and operative mortality in cancer surgery: a national study. Arch Surg 2003;138:721–725. discussion 726. [PubMed: 12860752]

70. Elshaikh M, Ljungman M, Ten Haken R, Lichter AS. Advances in Radiation Oncology. Annu Rev Med. 2005

71. Gabizon AA. Pegylated liposomal doxorubicin: metamorphosis of an old drug into a new form of chemotherapy. Cancer Invest 2001;19:424–436. [PubMed: 11405181]

72. Kamaly N, Kalber T, Ahmad A, Oliver MH, So PW, Herlihy AH, Bell JD, Jorgensen MR, Miller AD. Bimodal paramagnetic and fluorescent liposomes for cellular and tumor magnetic resonance imaging. Bioconjug Chem 2008;19:118–129. [PubMed: 17985841]

73. Zalipsky S, Saad M, Kiwan R, Ber E, Yu N, Minko T. Antitumor activity of new liposomal prodrug of mitomycin C in multidrug resistant solid tumor: insights of the mechanism of action. J Drug Target 2007;15:518–530. [PubMed: 17671898]

74. Booser DJ, Esteva FJ, Rivera E, Valero V, Esparza-Guerra L, Priebe W, Hortobagyi GN. Phase II study of liposomal annamycin in the treatment of doxorubicin-resistant breast cancer. Cancer Chemother Pharmacol 2002;50:6–8. [PubMed: 12111105]

75. Zou Y, Priebe W, Perez-Soler R. Lyophilized preliposomal formulation of the non-cross-resistant anthracycline annamycin: effect of surfactant on liposome formation, stability and size. Cancer Chemother Pharmacol 1996;39:103–108. [PubMed: 8995506]

76. Gros L, Ringsdorf H, Schupp H. Polymeric Anti-Tumor Agents on a Molecular and on a Cellular-Level. Angew Chem Int Edit 1981;20:305–325.

77. Savic R, Luo L, Eisenberg A, Maysinger D. Micellar nanocontainers distribute to defined cytoplasmic organelles. Science 2003;300:615–618. [PubMed: 12714738]

78. Matsumura Y, Kataoka K. Preclinical and clinical studies of anticancer agent-incorporating polymer micelles. Cancer Sci 2009;100:572–579. [PubMed: 19462526]

79. Nakanishi T, Fukushima S, Okamoto K, Suzuki M, Matsumura Y, Yokoyama M, Okano T, Sakurai Y, Kataoka K. Development of the polymer micelle carrier system for doxorubicin. J Control Release 2001;74:295–302. [PubMed: 11489509]

80. Satomi T, Nagasaki Y, Kobayashi H, Otsuka H, Kataoka K. Density control of poly(ethylene glycol) layer to regulate cellular attachment. Langmuir 2007;23:6698–6703. [PubMed: 17480105]

81. Matsumura Y, Hamaguchi T, Ura T, Muro K, Yamada Y, Shimada Y, Shirao K, Okusaka T, Ueno H, Ikeda M, Watanabe N. Phase I clinical trial and pharmacokinetic evaluation of NK911, a micelle-encapsulated doxorubicin. Br J Cancer 2004;91:1775–1781. [PubMed: 15477860]

82. Wiernik PH, Schwartz EL, Strauman JJ, Dutcher JP, Lipton RB, Paietta E. Phase I clinical and pharmacokinetic study of taxol. Cancer Res 1987;47:2486–2493. [PubMed: 2882837]

83. Kim TY, Kim DW, Chung JY, Shin SG, Kim SC, Heo DS, Kim NK, Bang YJ. Phase I and pharmacokinetic study of Genexol-PM, a cremophor-free, polymeric micelle-formulated paclitaxel, in patients with advanced malignancies. Clinical Cancer Research 2004;10:3708–3716. [PubMed: 15173077]

84. Kim TY, Kim DW, Chung JY, Shin SG, Kim SC, Heo DS, Kim NK, Bang YJ. Phase I and pharmacokinetic study of Genexol-PM, a cremophor-free, polymeric micelle-formulated

paclitaxel, in patients with advanced malignancies. Clin Cancer Res 2004;10:3708–3716. [PubMed: 15173077]

85. Hirsch LR, Stafford RJ, Bankson JA, Sershen SR, Rivera B, Price RE, Hazle JD, Halas NJ, West JL. Nanoshell-mediated near-infrared thermal therapy of tumors under magnetic resonance guidance. Proc Natl Acad Sci U S A 2003;100:13549–13554. [PubMed: 14597719]
86. Loo C, Lin A, Hirsch L, Lee MH, Barton J, Halas N, West J, Drezek R. Nanoshell-enabled photonics-based imaging and therapy of cancer. Technol Cancer Res Treat 2004;3:33–40. [PubMed: 14750891]
87. Serda RE, Gu J, Bhavane RC, Liu X, Chiappini C, Decuzzi P, Ferrari M. The association of silicon microparticles with endothelial cells in drug delivery to the vasculature. Biomaterials 2009;30:2440–2448. [PubMed: 19215978]
88. Serda RE, Ferrati S, Godin B, Tasciotti E, Liu X, Ferrari M. Mitotic partitioning of silicon microparticles. Nanoscale 2009;2:173–288.
89. Serda RE, Gu J, Burks JK, Ferrari K, Ferrari C, Ferrari M. Quantitative mechanics of endothelial phagocytosis of silicon microparticles. Cytometry A 2009;75:752–760. [PubMed: 19610127]
90. Sakamoto JH, van de Ven AL, Godin B, Blanco E, Serda RE, Grattoni A, Ziemys A, Bouamrani A, Hu T, Ranganathan SI, De Rosa E, Martinez JO, Smid CA, Buchanan RM, Lee SY, Srinivasan S, Landry M, Meyn A, Tasciotti E, Liu X, Decuzzi P, Ferrari M. Enabling individualized therapy through nanotechnology. Pharmacol Res. 2010

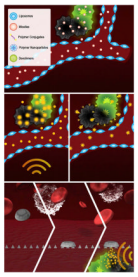

Figure 1.
The schematic representation of three generations of nanovectors shows first generation vectors with passive tumor targeting by means of EPR (top), followed by externally activated (A) or actively targeted (B) second generation vectors (middle), and multi-functional, third generation vectors comprised of multiple components that perform time-sequences of events (bottom). Reproduced from Sakamoto *et al* [90] courtesy of Elsevier.

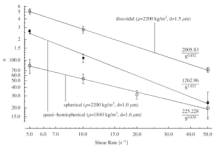

Figure 2.
Flow chamber determination of the number of particles (n), based on shape, marginating towards endothelial cells per second as a function of shear rate. Discoidal particles marginate at the highest frequency for all shear rates, followed by quasi-hemispherical particles, and then spherical particles. Reproduced from Gentile *et al.* [40], courtesy of Elsevier.

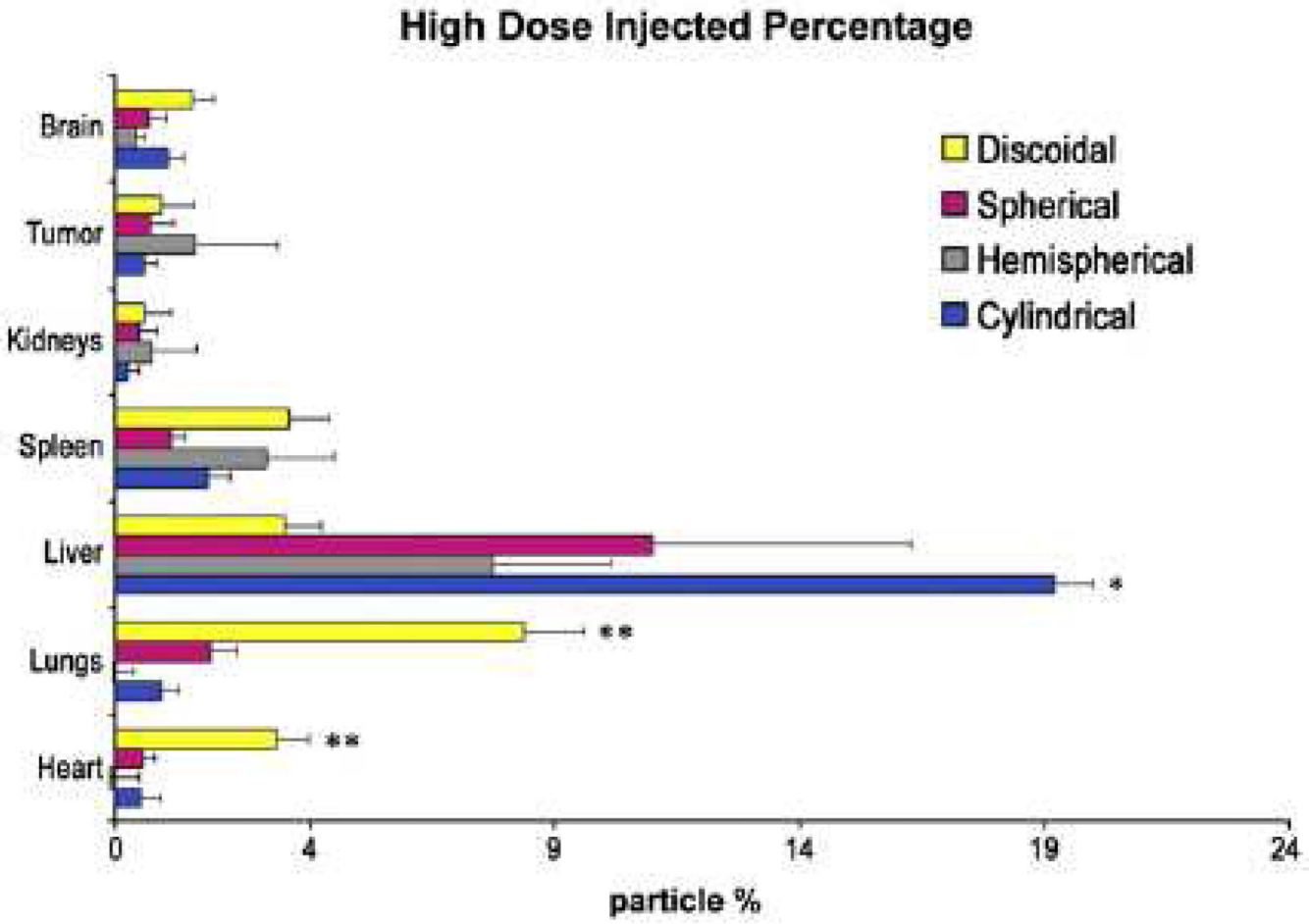

Figure 3.
Tissue distribution of silicon relative to the injected dose of silicon microparticles. The percentage of silicon is reflective of the number of particles of various shapes accumulating in each organ 6 hrs after intravascular injection of microparticles into mice containing orthotopic breast tumors. Reproduced from Decuzzi *et al.*[43], courtesy of Elsevier.

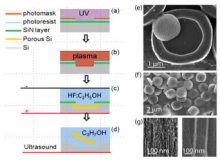

Figure 4.

Outline of the fabrication protocol for porous silicon particles (a–d) and SEM micrographs of the resulting particles (e–g). (a) A silicon substrate masked with silicon nitride is patterned through photolithography; (b) trenches are formed in the silicon by reactive ion etch; (c) the trenches are selectively porosified by electrochemical etch in a solution of hydrofluoric acid and ethanol; (d) the particles are released from the substrate by sonication in isopropanol; (e) backside of a 1.6 μm particle laying on the external corona of a 3.2 μm particle; (f) overview of a collection of 3.2 μm discoidal particles. (g) left: typical porous structure ranging from 10 to 20 nm; right: typical porous structure for pores larger than 20 nm.

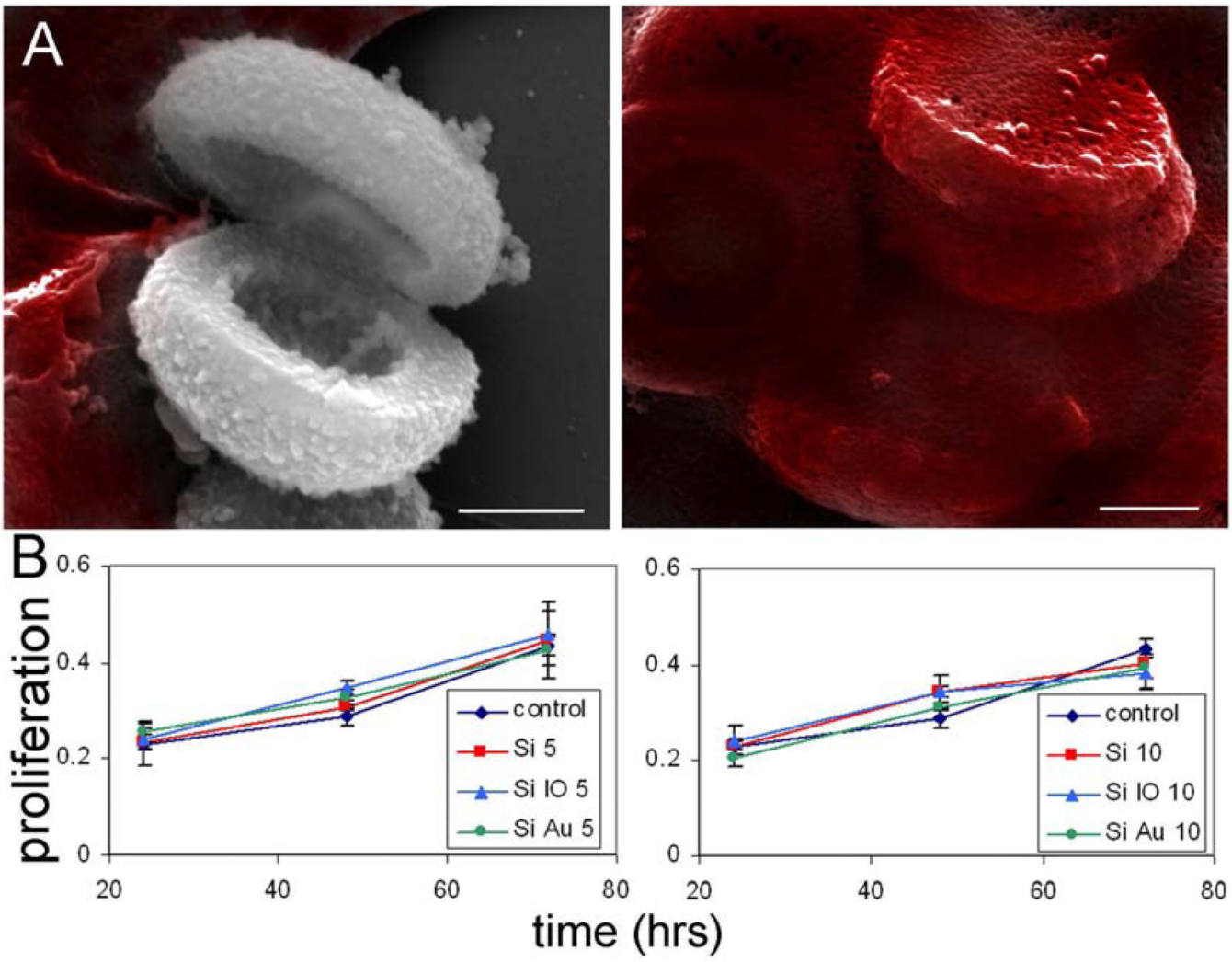

Figure 5.

Biocompatibility of porous silicon microparticles. A) Scanning electron micrographs show endothelial binding (left) and internalization (right) of silicon (Si) microparticles loaded with gold nanoparticles (scale bars 1 μm). B) Endothelial proliferation (formazan absorbance at 570 nm) is unaffected by either control or nanoparticle [iron oxide (IO) or gold (Au)] loaded silicon microparticles (left 5:1; right 10:1; particles:cells). Adapted from Serda et al. [88], courtesy of RSC Publishing.

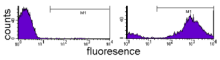

Figure 6.
Loading of annamycin liposomes into porous silicon microparticles. Fluorescence associated with hemispherical nanoporous particles before (left panel) and after (right panel) loading.

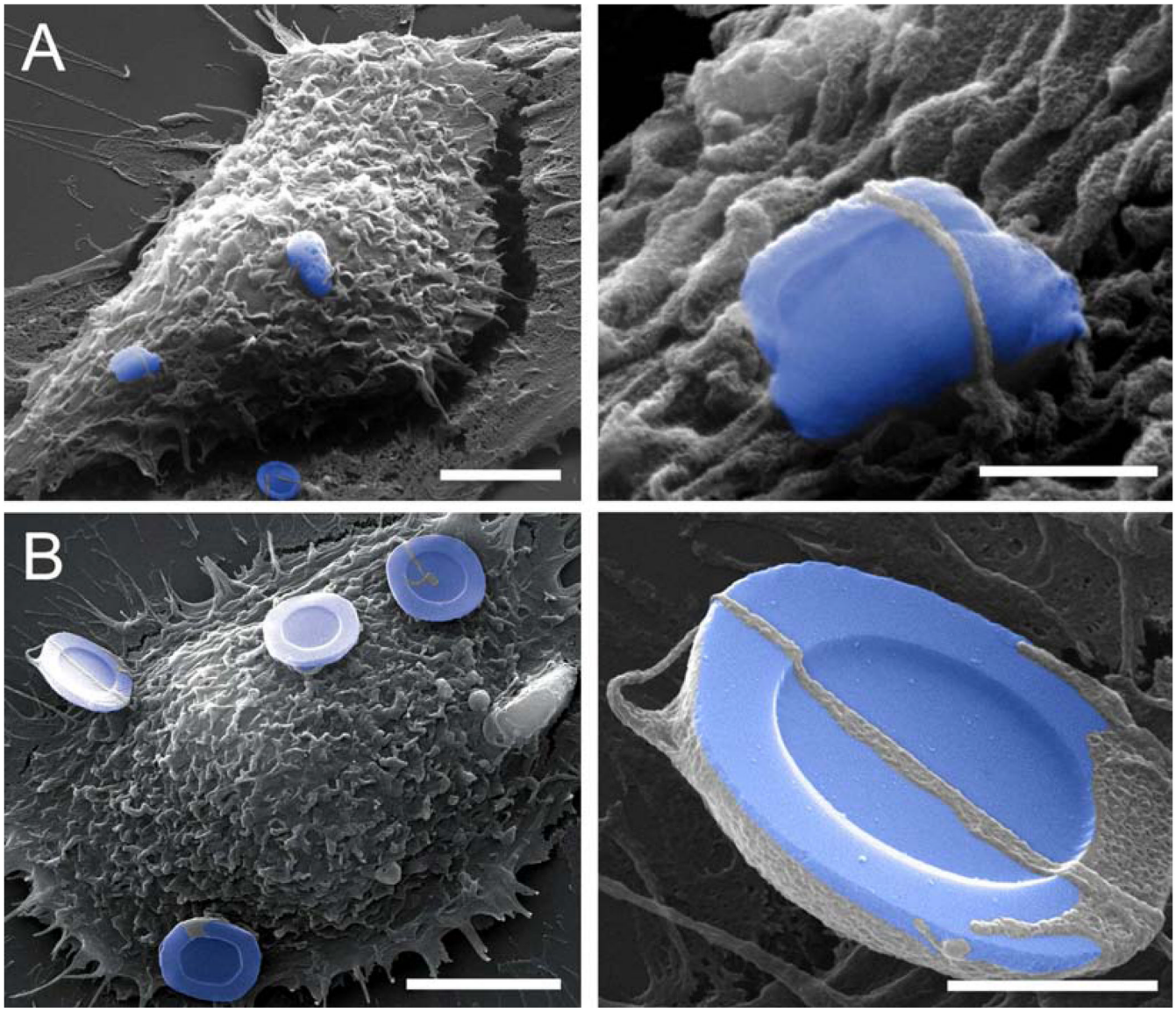

Figure 7.
Scanning electron micrographs show endothelial binding and engulfment of 1.6 μm (top row) and 3.2 μm (bottom row) silicon microparticles [bars 5 μm (left) and 1 μm (right)]. Reproduced from Serda et al. [88], courtesy of RSC Publishing.

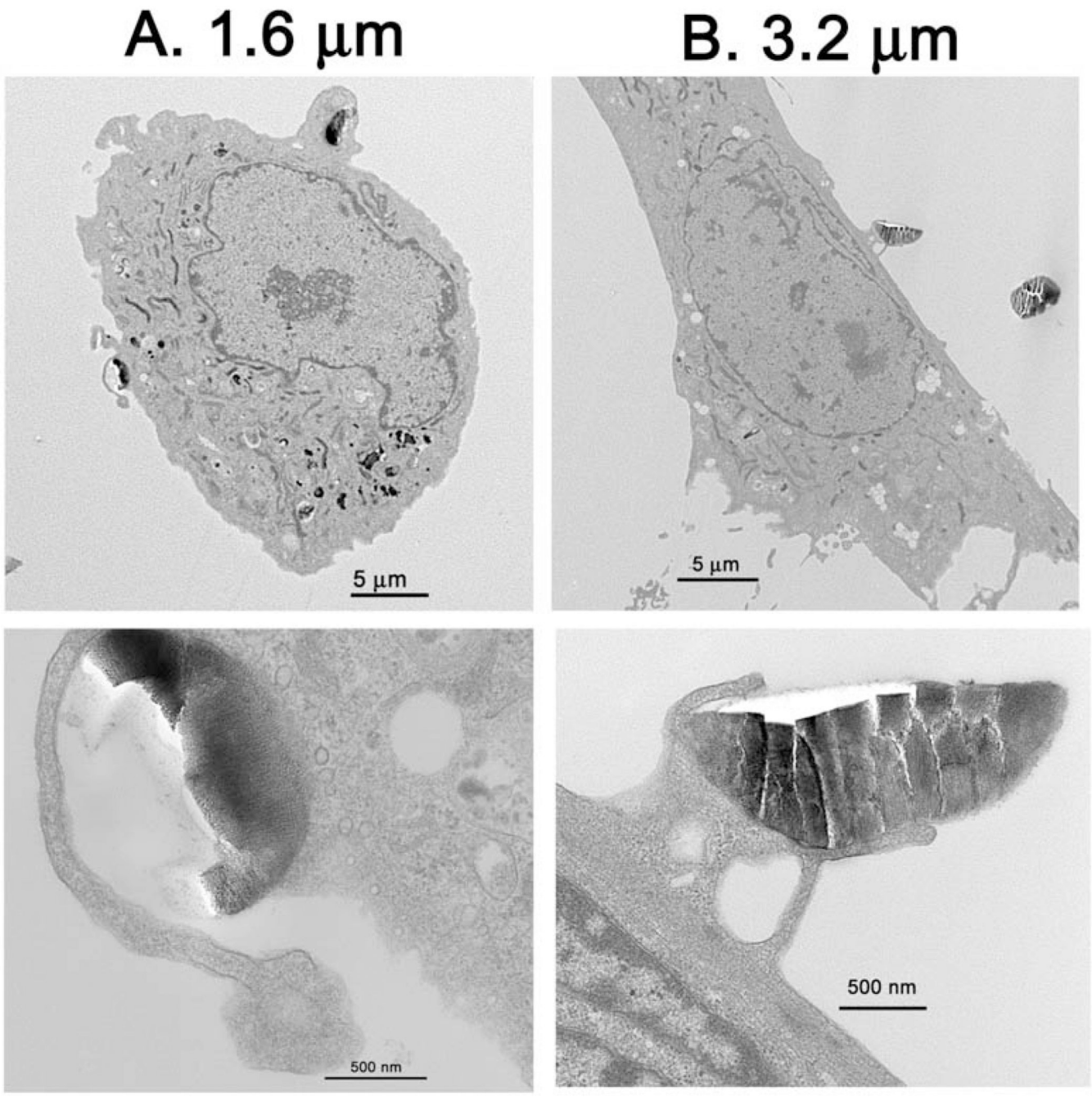

Figure 8.
Endothelial cells internalize silicon microparticles by rearrangement of the actin cytoskeleton. Transmission electron micrographs show internalization of larger, 3.2 µm particles by phagocytosis (A) and smaller, 1.6 µm, particles by macropinocytosis (B). Adapted from Serda et al. [87], courtesy of Elsevier.

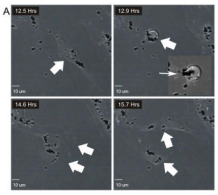

Figure 9.
Endothelial cells undergo mitosis with equal partitioning of silicon microparticle-encapsulated endosomes between the daughter cells, as captured by real-time confocal imaging. Adapted from Serda et al. [88], courtesy of RSC Publishing.